DOI: 10.2195/lj_Proc_ajmal_en_201912_01
URN: urn:nbn:de:0009-14-49946

Detailed analysis of cohesive DEM parameter fields using Uniaxial Rapid Flow Low Consolidation test for calibration of cohesive bulk materials

Detaillierte Analyse der Parameterfelder zur Kalibrierung von kohäsiven Schüttgütern mittels Uniaxial Rapid Flow Low Consolidation Tests

Mohsin Ajmal
Thomas Rößler
André Katterfeld

Lehrstuhl Förder- und Materialflusstechnik
Fakultät Maschinenbau, Institut für Logistik und Materialflusstechnik
Otto-von-Guericke-Universität

Discrete Element Method (DEM) is a broadly accepted and well established tool for simulating bulk materials. However, cohesion and adhesion is one field of DEM where a lot of questions still remain unanswered. One of the methods employed to answer this question is calibration and validation, by performing a detailed study of the DEM parameter fields and comparing them with experimental results, in order to zero in on a unique set of parameters which satisfy the experimental results.

[Keywords: Cohesion, JKR model, Discrete Element Method, DEM, Calibration]

A lot of contact models exist which explain cohesion in their own unique ways, however, JKR model is widely used for cohesive simulations due to its robustness and a relatively wide area of application. The JKR model tackles cohesion by introducing Surface Energy Density and increased particle overlap. Cohesive DEM simulations were performed using a combination set of Friction coefficients, Young's Modulus and Surface Energy Density. These were then compared with the reference experiments to narrow down on a specific set of parameters. Hence a systematic analytically driven calibration protocol will be established which can be used to calibrate different other cohesive materials. Further investigations will be carried out to assess the effect of cohesion and adhesion on rolling resistance.

Various parameter calibration and validation endeavours in recent years have been quite successful in answering those questions on a macroscopic level. In this work a Draw Down setup, rightly classified as Uniaxial Rapid Flow Low Consolidation test, was chosen to study the cohesive behavior of under study materials. One of the draw-backs of calibration is that a very large number of simulations should be performed to have an acceptable result. For this purpose, High Performance Cluster (HPC) computing is a valuable asset. In this exercise the simulations were done using highly parallel computing ability of ''OvGU HPC Neumann''. Parallel computing greatly reduces the time required for the whole exercise, which otherwise would have been deemed too computationally intensive to undertake.

[Schlüsselwörter: Cohesion, JKR modele, Diskrete Elemente Methode, DEM, Kalibrierung]

1 INTRODUCTION

Characterization of bulk materials for the design of material handling equipment is an active field of research, with focus ranging from computational to experimental approaches for the evaluation of widely used industrial materials. Further complications arise when cohesive bulk materials are under study. Cohesive materials are especially difficult to handle, therefore significant problems occur in industry due to blockages in equipment such as hoppers, chutes, feeders and conveyors. Designing and the optimisation of processes and equipment becomes quite difficult due to the lack of understanding of the cohesion and adhesion phenomenon, which may also lead to inefficient handling and transport techniques.

By making use of DEM efficient bulk solid handling equipment can be designed or existing ones can be optimised as demonstrated by [CRWMP17]. DEM models for industrial applications are typically idealized in terms of

DOI: 10.2195/lj_Proc_ajmal_en_201912_01
URN: urn:nbn:de:0009-14-49946

the considered particle size, shape and stiffness. Due to this idealisation, calibration in DEM is required, in which a carefully chosen parameter field is analysed thoroughly and systematically. Ambiguous properties such as particle-to-particle friction, rolling friction, and additional cohesive properties must be defined for DEM simulations. Calibration exercises try to bridge the gap between idealization and reality by comparing experimental results with simulations, which are conducted over a carefully chosen parameter field. A matching response between simulations and experiments can be found in this way, allowing to implement the narrowed down ambiguous parameter set in real world applications with satisfactory results.

Valuable work in the field of calibration and validation has been undertaken by [GK06], [GW11], [Coe16], [RRKW19] and [RK19]. One of the major draw backs of this approach is that it involves a lot of trial and error, henceforth a large number of simulations are required. HPCs are therefore a valuable tool to run several simulations in parallel. This allows for a thorough analysis of the parameter fields. Implementation of optimization and A.I algorithms ([RH17], [DAS18], [RKRW18]) and the general advancement in processing power. Advancements in the implementation of A.I. algorithms as shown by [BKP16], can further reduce the simulations required for calibration, allowing for the analyses of more refined parameter fields in significantly less time.

In the mentioned application ranges of bulk material handling, often rapid material flow can be observed with low consolidation. The calibration approach should consider these boundary conditions. [RRKW19] proposed a standardized calibration procedure for cohesion less bulk materials by using iso-plots and limiting the ranges of iso-plots to the experimental error. They also discussed in detail the problem of ambiguous parameter sets. [CWWKENC18] uses a similar experimental approach which narrows down on a unique set of parameters for cohesive bulk materials. The approach proposed in this research uses a calibration strategy, albeit computationally demanding, to narrow down on a unique set of parameters by using iso- or contour- plots. Further analyses of the SJKR model is made to understand the limitations of this contact model and to specify cases in which it is not feasible to implement this contact model.

This paper focuses on developing a calibration protocol for cohesive bulk materials like wet sand using a draw down experiment. This gives a good indication about material flow regimes through openings of different sizes and the resulting angle of repose. The response of the experimental setup was calibrated against DEM simulations, with an aim to narrow down on a set of parameters which mimic the experimental results. It was also observed that at smaller opening sizes the material was unable to flow, resulting in arching at the opening. This arching and free flow phenomenon gives some insight into the clogging behavior of cohesive bulk materials, as one of the biggest problems about cohesive bulk handling is its high susceptibility to block the equipment and in case of continuous processes resulting in the shut-down of the operation and lost revenue. Wet sand is chosen as the bulk material with a Moisture Content (MC) of 10% for the experimental measurements.

2 METHODS AND MODELS

2.1 CONTACT MODELS

As in most DEM simulations, the Hertz-Mindlin contact model is used and rolling friction is according to [WK12]. The choice of time step is critical as it can have a profound effect on the simulation behavior. 15% of Rayleigh time is generally chosen as the simulation time step, as it is a very widely used and well-established criterion for DEM simulations.

Parameter	Value	Description
Contact models		Hertz-Mindlin
		SJKR
		Modified elastic plastic spring
		dashpot model , [WK12]
Particle density (kg/m^3)	2083	Experiment
Young's Modulus (Pa)	1E8	Aproximation; reduction
Poisson's ratio	0.3	Approximation
Coefficient of restitution	0.2	Approximation
Particle-wall friction coefficient	0.41	Experiment
Time step (s)		15% of Rayleigh time
Gravity (m/s^2)	9.81	Global value

Figure 1. Parameters and model Selection for DEM Simulations

2.2 THE JOHNSON KENDEL AND ROBERTS (JKR) MODEL

[JKR71] tried to explain cohesion on the basis of surface energy density while others used liquid bridging between particles and the capillary force to develop models which describe cohesive behavior of substances, such as the method proposed by [SM08]. Others, such as [EW13], tried to develop a cumulative approach by using a combination of different models. Substances with particle sizes in the range of micrometers or nanometers are more influenced by intermolecular forces such as Van-der-Waals forces and electrostatic forces than macro particles from millimeter to centimeter range, which are generally more effected by material bridging, as shown in Table 2. It becomes quite challenging to quantify each and every phenomenon in one effort as the variable count becomes quite large and the subsequent computational cost will increase to impractical scales. Before the start of each simulation effort it therefore becomes quite a necessary exercise to identify the major cohesion mechanism of the under-study material.

DOI: 10.2195/lj_Proc_ajmal_en_201912_01
URN: urn:nbn:de:0009-14-49946

Table 1. Cohesion Mechanism ([Rum16])

Without material bridges	With material bridges	
	Liquid bridges	Solid Bridges

• Electrostatic interaction	• Free moveable liquid surface
	  ○ Capillary Forces
	  ○ Interfacial Forces
		• Sintering

• Van-der-Waals Forces	• Not moveable binder bridges	• Grain Growth
• Valence bond	○ Binder ○ Glue ○ Absorption Forces	• Crystallization

[JKR71] developed a model in 1971 which further extends the Hertz model to take into account the effect of tensile forces at the contact area edges in order to explain the cohesive behavior. This approach is unique in a sense that it tries to explain cohesion without the effect of moisture and material bridging, hence making it quite suitable to explain the sticking behavior of microscopic dry matter such as dust and powders. During various experiments they observed that a contact is maintained between particles without the presence of an external force. According to this model the total force, F_{all} acting at the contact point of the two particles is given by:

$$F_{all} = F_{ext} + 3\gamma\pi R + \sqrt{3\gamma\pi R F_{ext} + (3\gamma\pi R)^2} \quad \text{Eq.1}$$

Where, F_{ext} is the external normal force acting on the particle, γ is the cumulative surface energy density, and R is the effective radius for the particle radii R1 and R2. The radius of contact a as proposed by JKR theory becomes:

$$a^3 = \frac{R}{K}(F_{ext} + 3\gamma\pi R + \sqrt{6\gamma\pi R F_{ext} + (3\gamma\pi R)^2} \quad \text{Eq.2}$$

The cumulative surface energy is given by:

$$\gamma = \gamma_1 + \gamma_2 - 2\gamma_{12} \quad \text{Eq.3}$$

here, γ_1 and γ_2 are the intrinsic surface energies (J/m2) of the two particles and γ_{12} is the interfacial energy. A combining law for Van-der-Waals interaction is given by; $\gamma_{12} = \sqrt{(\gamma_1 \times \gamma_2)}$. With an attractive surface energy, a force is required to separate the spheres even if no external force is present.

$$F_c = 3\pi\gamma R \quad \text{Eq.4}$$

This work of cohesion or pull force, Fc, is independent of the elastic contact properties of the particles. When taking into account the surface energy at contact this model predicts that the force at the contact is changed from Hertzian contact to a more cohesive contact and further evaluation of the force distribution leads to the following equation describing the normal and adhesive contact between particles, as outlined in the work of [CTH93].

$$F = \frac{4Ea^3}{3R} - 2\pi a^2\sqrt{\frac{4\gamma E}{\pi a}} \quad \text{Eq.5}$$

Simplified models are often used in DEM which reduce the time required to simulate large industrial cases, where it can be assumed that the effect of simplification will not be prohibitively profound. One of the most commonly used models is the simplified JKR models which is implemented in the open-source DEM code LIGGGHTS®. This simplified approach reduces the computational time by combining together surface energy, young's modulus and contact radius into one parameter 'Cohesion Energy Density (CED)'. Investigations prior to this work have shown that with high CED values and low Young's modulus the particles implode into each other leading to highly unstable systems. This may be due to the fact that a reduction in stiffness of the particles is unable to counteract the effects of high attractive forces leading to unrealistic overlaps. A relation given by [HKWSJSC27] explains the reduction of surface energy with respect to young's modulus which is given by:

$$\gamma_{mod} = \gamma\left(\frac{E_{mod}}{E}\right)^{2/5} \quad \text{Eq.6}$$

Where γ_{mod} is the modified surface energy (J/m2) and E_{mod} is the modified young's modulus. Since the concept of CED is completely different from surface energy, Eq. (6) cannot be applied in this regard. Our previous investigations have shown that with using the CED of the SJKR model, young's modulus should be a minimum of 1E8, in order to avoid implosive instability of a system. Although approaches using CED are applicable in some instances, but with rapid flow and high consolidations this approach leads to the same instabilities previously mentioned, limiting us to remain in the realm of low consolidations. This can be improved by further improving this simplified approach by taking into account the changing contact radius with each time step. This improvement may allow for an explanation of the unstable behavior of the system at low young's modulus and high surface energies.

3 EXPERIMENTAL SETUP

A draw-down experimental set-up, as proposed by [CRKW18], [RRKW18], [CWWKENC18], was used for the calibration of wet sand. It consists of two boxes made of Perspex, their dimensions are shown in Figure 1. The depth of the top box is 100mm and the lower box is 180mm. Flaps are installed at the bottom opening of the top box, which can be opened instantaneously, so that the material flows un-obstructed from the top box and the errors related to delayed opening can be reduced. To measure the flow rate of the material from the top box, it is placed on load cells. As the material flows out from the top box a shear angle is formed in the top box, while a heap is

DOI: 10.2195/lj_Proc_ajmal_en_201912_01
URN: urn:nbn:de:0009-14-49946

formed at the bottom which is a good indication of the angle of repose. The material under investigation was filled up to a height of 300mm in the top box. The shear angle (degree), φ_{DD}, in the top box and the angle of repose (degree), β_{DD}, in the bottom box were measured through image analysis. Each experiment was repeated three times. In Table 3, the results of the experiments are presented.

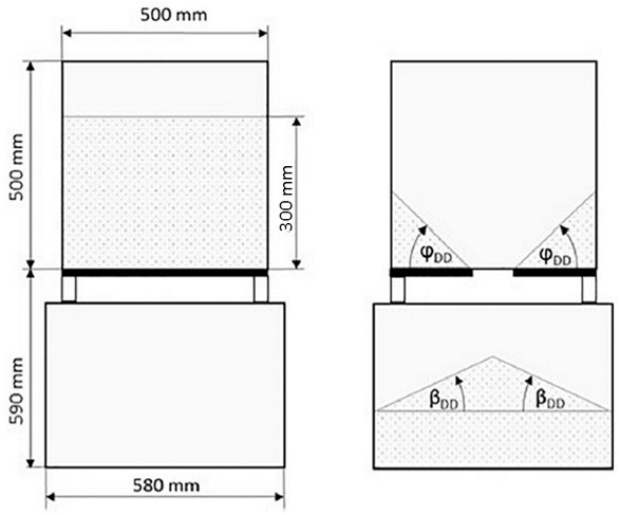

Figure 2. Schematic of draw down apparatus.

Table 2. Experimental Results

	Angle of Repose β_{DD} (AOR) [degree]	Mass loss [kg]
Opening 90 mm	1.75	0.47
Opening 120 mm	28.7	7.23
Opening 150 mm	30.1	7.79

4 DEM Parameter Calibration

4.1 Simulation Setup

The simulations for parameter calibration were undertaken using the open-source software LIGGGHTS®. An up-scaling approach was used to simulate wet sand, as it is not practically possible to simulate sand with its real particle size ranges (see Figure 2). A scaling factor of 10 was used in this application as the diameter of the largest particle was still approximately 10 times smaller than the opening size in the top box, which assures that unrealistic blocking will not occur during simulations.

The calibration procedure was undertaken using a parameter field of μ_{p-p}(particle-to-particle friction), μ_r (coefficient of rolling friction), CED and Adhesion Energy Density (AED). AED values for the particle-to-wall contact were the same as the CED values in order to reduce the number of simulations, however according to our understanding AED has an effect on the results and should be investigated further. The calibration was undertaken according to the procedure outlined in Figure 3. From the experimental measurements, the mass-loss in the top box and the angle of repose in the bottom box were measured and set as the reference values. The parameter field was systematically varied in order to narrow down to a set which is in good agreement with the experimental results.

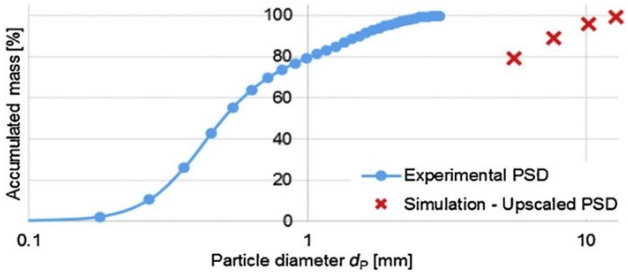

Figure 3. Particle size distribution comparison.

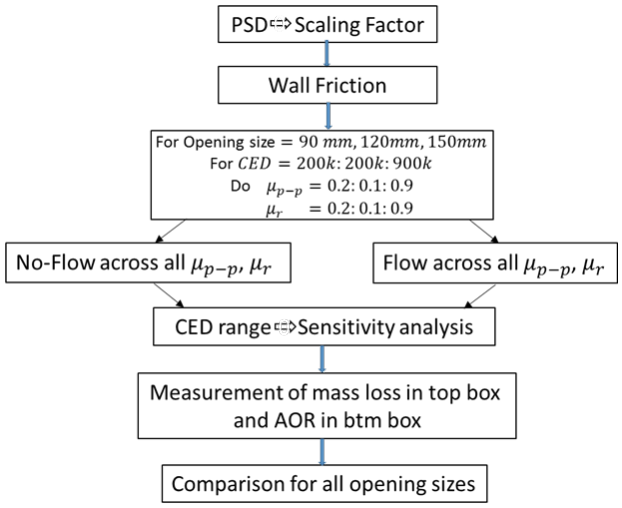

Figure 4. Calibration protocol using the draw down testing apparatus

Every simulation was undertaken with an up-scaled particle count of approximately 95000 particles. The simulation time was set to a constant 6 seconds. Simulations for opening sizes of 90 mm and 150 mm were performed, which were similar to the experimental measurements. Later the same simulation approach was applied to opening size 120 mm to get more refined results for the developed approach. These were then compared together to get the best possible agreement. The simulation parameters are shown in Table 1.

4.2 DEM Simulation Results

A large number of DEM simulations were performed so as to have a very thorough understanding of the parameter influence. Approximately, 1500 simulations were performed on the HPC cluster Neumann of the University of Magdeburg in order to analyze all parameter sets. In this way it is possible to narrow down on a unique set which defines the up-scaled particles. All the parameters, which were investigated have a profound influence on the results.

DOI: 10.2195/lj_Proc_ajmal_en_201912_01
URN: urn:nbn:de:0009-14-49946

In order to get a limit on CED values, the point where no flow or blocking in the top box and sure flow were analysed. The values of CED corresponding to no flow and sure flow were taken as the lower and the upper limits respectively. A sensitivity analysis between these limits was then undertaken in order to narrow down on the value of CED for which result in an overlap agreement for all possible parameter combinations. The lower limit corresponds to the phenomenon when there is flow from the opening sizes of 120 mm and 150 mm at all combinations of μ_{p-p} and μ_r. In the experiments mass loss from these opening sizes and arching at opening sizes of 90 mm and below were recorded. This criteria can be different for different materials and should be investigated in the experiments. The upper limit on the other hand shows no flow or arching at even the lowest possible combination of μ_{p-p} and μ_r.

It was further observed that changing AED values also led to differences in the material behavior inside the apparatus. This strengthens our understanding that wall effects also play a major role in the flow or the loss of material from the top box.

Figure 4 shows the results of mass loss in the top box and angle of repose AOR for CED 700000 for the three opening sizes. The AOR in simulation was measured with the same algorithm used in [RK19]. The limits of the highlighted areas in the contour plots were chosen ±10% of the average experimental values.

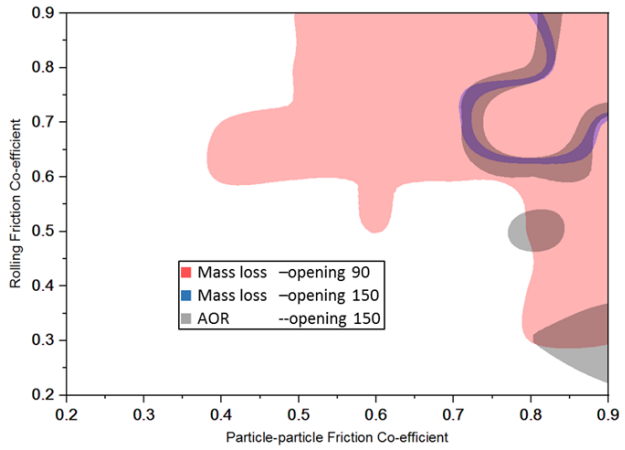

Figure 5. Contour plot for a 150 mm opening.

The simulations undertaken in the first phase resulted in similar contour areas for mass loss and angle of repose for an opening size of 150 mm. The red area shows the region where arching occurs with an opening size of 90 mm. The overlaying of result for two opening sizes with repeatable arching and outflow behavior shows that based on these two tests it is not possible to identify a single parameter set which results in the same mass loss and AOR.

In order to get a more refined area of our parameter set the same simulations were repeated for an opening size of 120 mm (see Figure 6). Overlapping these two plots results in a common area which can be identified as the best possible solution for the three opening sizes. In this way it was found possible that a unique set of parameters can be identified which fit most of the scenarios for the SJKR model. Figure 7 shows a common overlap area (marked by red circle in bottom figure) at approximately μ_{p-p}=0.7 and μ_r=0.8 is observed, giving the required parameter set for wet sand calibration. Figure 8 shows the direct comparison of experimental and simulation results via images of the draw down test after the flow of the material has finished.

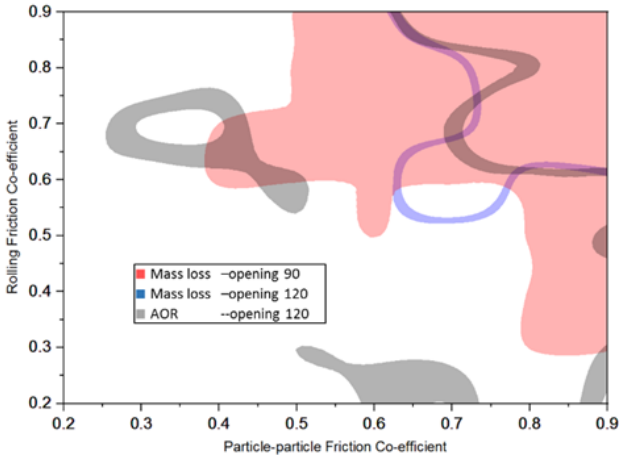

Figure 6. Contour plot for opening 120 mm

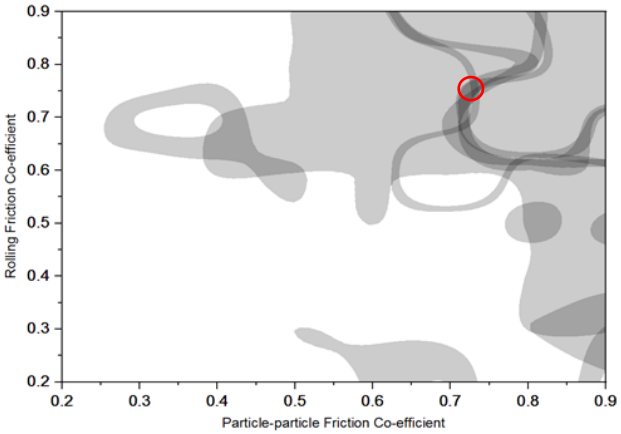

Figure 7. Overlap of plots of opening 120 mm and 150 mm.

DOI: 10.2195/lj_Proc_ajmal_en_201912_01
URN: urn:nbn:de:0009-14-49946

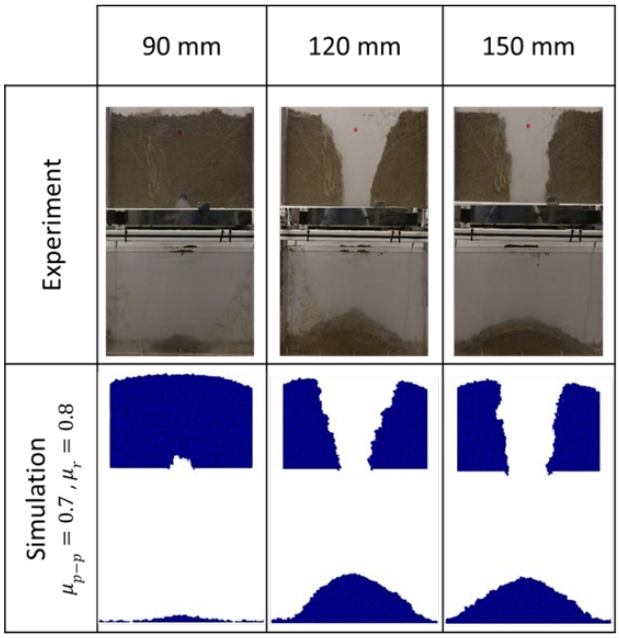

Figure 8. Comparison of experimental and simulation results for the acquired best fitted parameter set (CED=700k J/m3).

Table 3 shows the comparison between experimental and simulation results for the obtained parameter set.

Table 3. Experimental vs Simulation values

	Mass loss (kg)		Shear Angle (degree)		Angle of repose (degree)	
Opening size (mm)	Experimental	Simulation	Experimental	Simulation	Experimental	Simulation
90	0.47	0.43	N/A	N/A	1.75	1.25
120	7.23	8.36	78.57	77.49	28.7	40.35
150	7.79	8.77	84.51	83.03	30.1	35.1

The experimental and simulation regime was undertaken using a low consolidation approach. High consolidated cohesive materials behave similar to a solid structure, which is very difficult to simulate and quantify. Efforts are made to avoid consolidation of bulk material in practical applications, however it is quite difficult to prevent. A thorough study has been undertaken in this work to analyse all possible parameters which can contribute to an eventual progress towards consolidation of cohesive bulk material in practical application, allowing us to avoid this eventuality.

5 CONCLUSION

From the obtained results it is clear that a satisfactory agreement for simulations and experiments was achieved. However, it also became clear, that an increase number of tests (at least 3) with different opening sizes is necessary to achieve a single parameter set. Draw down experimental measurements can therefore be used not only for cohesionless bulk materials but also to calibrate cohesive materials using the SJKR model. The following examinations would be beneficial in terms of improving and further validating the presented method.

- Other cohesive contact models such as the Edinburgh Elasto-Plastic Adhesion ‘EEPA’ contact model and ‘Easo’ liquid bridging contact models are available in LIGGGHTS® which can also be studied in this context, especially in the area of partical-wall adhesion
- Implementation and study of the JKR model in its entirety, albeit for the narrowed down parameter set.
- Study of further cohesive rolling resistance models.
- Study the effect of AED in detail.

LITERATURE

[CRWMP17] Chen, W., Roberts, A., Williams, K., Miller, J., & Plinke, J. (2017). On uniaxial compression and Jenike direct shear testings of cohesive iron ore materials. Powder Technology, 312, 184–193.

[GK06] Gröger, T.; Katterfeld, A.: On the Numerical Calibration of Discrete Element Models for the Simulation of Bulk Solids. Computer Aided Chemical Engineering 21. 2006

[GW11] Grima, A. P., Wypych, P. W. (2011). Development and validation of calibration methods for discrete element modelling. Granular Matter, 13(2), 127–132.

[Coe16] Coetzee, C. J. (2016). Calibration of the discrete element method and the effect of particle shape. Powder Technology, 97, 50–70.

[RRKW19] Roessler, T., Richter, C., Katterfeld, A., Will, F.: Development of a standard calibration procedure for the DEM parameters of cohesionless bulk materials–part I: Solving the problem of ambiguous parameter combinations, Powder Technology 343 (2019) 803–812

[RK19] Roessler, T., Katterfeld, A., DEM parameter calibration of cohesive bulk materials using a simple angle of repose test, Particuology 343 (2019) 803–812

DOI: 10.2195/lj_Proc_ajmal_en_201912_01
URN: urn:nbn:de:0009-14-49946

[RH17] Rackl, M., Hanley, K. J., A methodical calibration procedure for discrete element models. Powder Technology 307 (2017) 73–83.

[DAS18] Do, H.Q., Aragón, A.M., Schott, D.L., A calibration framework for discrete element model parameters using genetic algorithms, Adv. Powder Technol. 29 (2018) 1393–1403 Nr. 6, S.

[RRKW18] Roessler, T.; Richter C.; Katterfeld, A.; Will, F.: Standardverfahren zur multikriteriellen Kalibrierung von DEM-Parametern von kohäsionslosen Schüttgütern unter Verwendung eines Optimierungsalgorithmus. In: Fachtagung Schüttgutfördertechnik 2018. Technische Universität München, S. 53-76

[CRKW18] Chen, W., Roberts, A., Katterfeld, A., Wheeler, C., Modelling the stability of iron ore bulk cargoes during marine transport, Powder Technology 326 (2018), 255–26

[BKP16] Benvenuti, L., Kloss, C., & Pirker, S., Identification of DEM simulation parameters by Artificial Neural Networks and bulk experiments. Powder Technology 291 (2016) 456–465.

[CWWKENC18] Carr, M.; Wheeler, C.; Williams, K.; Katterfeld, A., Elphick, G.; Nettleton, K.; Chen, W.: Discrete element modelling of problematic bulk materials onto impact plates. In: CHoPS 2018: 9th International Conference for Conveying and Handling of Particulate Solids: at the Greenwich Maritime Campus, London, 10-14 September 2018 - London, insges. 6 S.

[WK12] Wensrich, C.; Katterfeld, A.: Rolling Friction as a Technique for Modelling Particle Shape in DEM. In: Powder technology. Volume 217, February 2012, Pages 409–417

[JKR71] Johnson, K. L., Kendall, K., Roberts, A. D, Surface energy and the contact of elastic solids. Proceedings of the Royal Society of London Series A 324 (1971) 301–313.

[SM08] Shi, D., McCarthy, J.J., Numerical simulation of liquid transfer between particles, Powder Technology 184 (2008) 64–75

[EW13] Easo, L. A., Wassgren, C. (2013) Comparison of liquid bridge volume models in DEM simulations. Retrieved from: https://aiche.confex.com/aiche/2013/webprogram/Paper312290.html

[Rum58] Rumpf, H. (1958). Grundlagen und methoden des granulierens. Chemie Ingenieur 660Technik, 30(3), 144–158

[HKWSJSC27] Hærvig, J.; Kleinhans, U.; Wieland, C.; Spliethoff, H.; Jensen A.L.; Sørensena, K.; Condra, T.J.; On the adhesive JKR contact and rolling models for reduced particle stiffness discrete element simulations, Powder Technology 319 (2017), 472-482

[CTH93] Chokshi, A., Teilens, A.G.G.M., Hollenbach, D., Dust Coagulation, The Astrophysical Journal 407 (1993) 809-819

Mohsin Ajmal, M.Sc., Research Assistant at the Chair of Conveying Technology, University of Magdeburg.

Address: Lehrstuhl Fördertechnik, Institut für Logistik und MaterialflusstechnikFakultät Maschinenbau, Otto-von-Guericke-Universität, Universitätsplatz 2, 39104 Magdeburg, Germany, Phone: +49 391-67-52690, Fax: +49 391-67-42646, E-Mail: mohsin.ajmal@ovgu.de

Thomas Rößler, M.Sc., Research Assistant at the Chair of Conveying Technology, University of Magdeburg.

Address: Lehrstuhl Fördertechnik, Institut für Logistik und MaterialflusstechnikFakultät Maschinenbau, Otto-von-Guericke-Universität, Universitätsplatz 2, 39104 Magdeburg, Germany, Phone: +49 391-67-52245, Fax: +49 391-67-12646, E-Mail: thomas.roessler@ovgu.de

André Katterfeld, Dr.-Ing., Professor of the Chair of Conveying Technology, University of Magdeburg.

Address: Lehrstuhl Fördertechnik, Institut für Logistik und MaterialflusstechnikFakultät Maschinenbau, Otto-von-Guericke-Universität, Universitätsplatz 2, 39104 Magdeburg, Germany, Phone: +49 391-67-58603, Fax: +49 391-67-42646, E-Mail: andre.katterfeld@ovgu.de